

Effect of phase transitions on liquid crystal colloids: a short review

Kottoli Poyil Zuhail, Matjaž Humar & Surajit Dhara

To cite this article: Kottoli Poyil Zuhail, Matjaž Humar & Surajit Dhara (2020) Effect of phase transitions on liquid crystal colloids: a short review, Liquid Crystals Reviews, 8:1, 44-57, DOI: [10.1080/21680396.2021.1904298](https://doi.org/10.1080/21680396.2021.1904298)

To link to this article: <https://doi.org/10.1080/21680396.2021.1904298>



Published online: 02 Apr 2021.



Submit your article to this journal [↗](#)



Article views: 46



View related articles [↗](#)



View Crossmark data [↗](#)



Effect of phase transitions on liquid crystal colloids: a short review

Kottoli Poyil Zuhail^{a,d}, Matjaž Humar^{a,b,c} and Surajit Dhara^d

^aJ. Stefan Institute, Ljubljana, Slovenia; ^bDepartment of Condensed Matter Physics, Faculty of Mathematics and Physics, University of Ljubljana, Ljubljana, Slovenia; ^cCENN Nanocenter, Ljubljana, Slovenia; ^dSchool of Physics, University of Hyderabad, Hyderabad, India

ABSTRACT

We present a brief review on the effect of phase transitions on liquid crystal colloids. The paper focuses on the evolution of dipolar, quadrupolar and boojum colloids and the ensuing elastic distortions of the director field across phase transitions between various phases, including N, SmA, SmC and N*. The role of pre-transitional and post-transitional elasticity on the resulting defect structure is discussed. Our review includes the results of structural transitions of two-dimensional colloidal assemblies due to the transformation of the defects across the phase transitions. Finally, we discuss some future perspectives on further studies.

ARTICLE HISTORY

Received 8 January 2021
Accepted 13 March 2021

KEYWORDS

Liquid crystals; colloids;
defects; phase transition

1. Introduction

Liquid crystals (LCs) are orientationally ordered fluids composed of shape anisotropic organic molecules. For rod-like molecules, the mean direction of the molecular orientation is defined by \hat{n} , a dimensionless unit vector [1]. LCs exhibit mesomorphic transitions and display an increasing degree of orientational and/or positional order with decreasing temperature. Nematic (N) phase is the least ordered and most fluid phase among all the known mesophases [1,2]. It is characterised by a long-range orientational order without any positional order. Many compounds exhibit nematic to smectic-A (N-SmA) phase transition, in which a one-dimensional positional order emerges in addition to the orientational order when the temperature is reduced to SmA phase. Several compounds also exhibit SmA to smectic-C (SmC) phase transition as the temperature is reduced in which the director \hat{n} tilts at an angle with respect to the layer normal. In cholesteric LCs (N*), the director shows a helical structure along with the long-range orientational order. This phase is observed when the molecules are inherently chiral or a chiral dopant is added to the ordinary NLC [3].

Dispersion of foreign particles in nematic liquid crystals (NLCs) creates elastic distortion of the director field \hat{n} which results in a topological defect in the neighbourhood of each particle [4–11]. When the particles are treated for perpendicular or homeotropic alignment of the director, they induce either a point-like hyperbolic hedgehog defect of strength -1 (Figure 1(a–c)) or

a ring-like defect (Figure 1(d–f)), so-called the Saturn ring defect of strength $-1/2$ in the medium. The particle-defect pairs are called elastic dipoles or quadrupoles in analogy with electric counterparts based on the similarity of electric field lines and the transverse components of the director field \hat{n} [7–9]. When the particles with planar surface anchoring of LC molecules are introduced in a planar cell, they create a pair of antipodal surface defects known as boojums (Figure 1(g–i)) [8,12–16].

The interaction potential between two elastic dipoles and quadrupoles are anisotropic and given by $U_{DD}(r, \theta) = C_1 K(1 - 3 \cos^3 \theta)/r^3$ and $U_{QQ}(r, \theta) = C_2 K(3 - 30 \cos^2 \theta + 35 \cos^4 \theta)/r^5$, respectively, where C_1 , C_2 are constants that depends on the particle size, K is the mean elastic constant of the LC, r is the separation between them and θ is the angle between the line connecting the centres of particles and the far-field orientation of the nematic director \hat{n} [8]. The long-range structural forces experienced by nematic colloids due to the elastic deformation obviously have no analogues in regular colloidal systems in an isotropic dispersive medium [17–23]. Exploiting these anisotropic forces and defects 2D [7] and 3D [24] structures of dipolar crystals have been demonstrated. Hence LC colloids are promising for creating new assemblies with complex architecture depending on the particles, surface anchoring and defects [25–30]. Here, by ‘colloids’ we mean the micrometre-sized particles having sedimentation length much larger than the isotropic counterpart due to the gradients of the director field that pushes the particles away from the bottom [31].

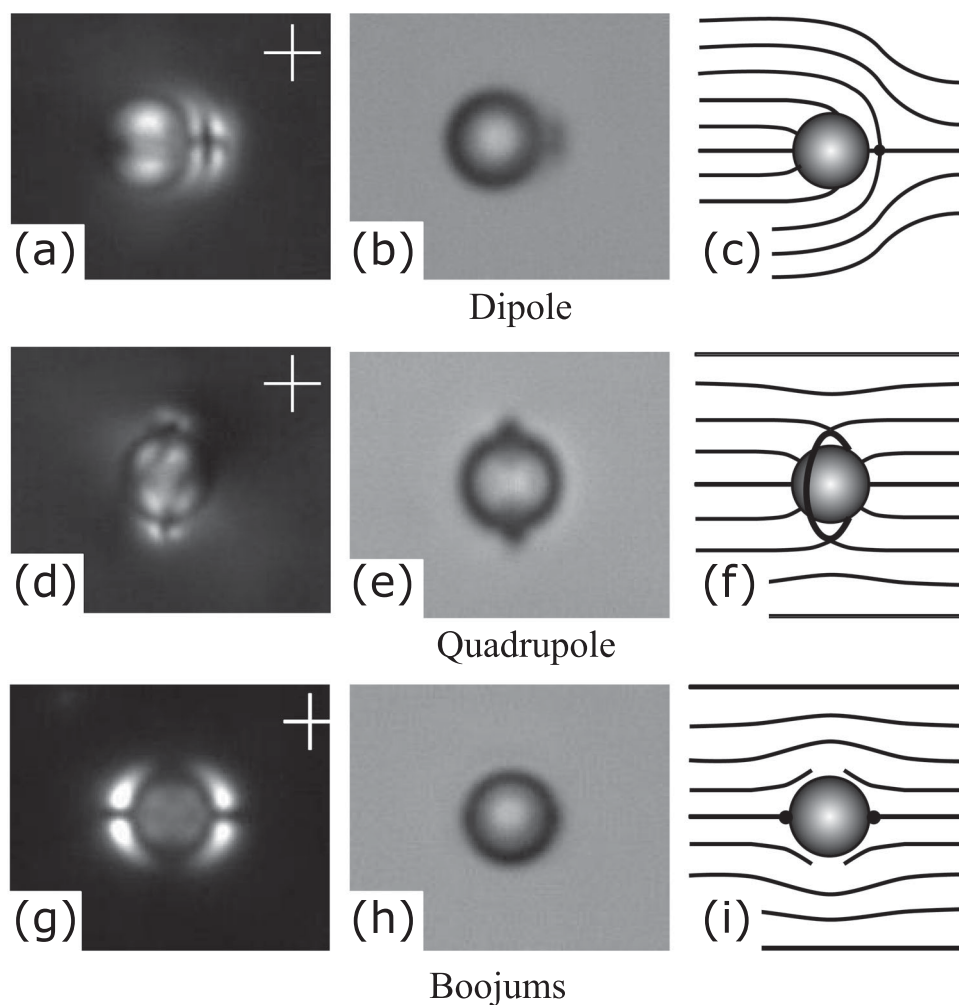


Figure 1. Polarising optical photomicrographs of (a) a dipolar, (d) quadrupolar and (g) a boojum colloid with the schematic director field are shown in (c,f,i). Bright field images of the respective colloids without crossed polarisers are shown in (b,e,h). Particle diameter is $5.2 \mu\text{m}$.

In this review, we discuss the effect of phase transitions on the topological defects induced by the colloidal particles across the phase transitions in LCs. We focus on elastic dipoles, quadrupoles and boojums in the nematic phase and the ensuing structures in the SmA and SmC phases. The experiments clearly bring out the role of temperature-dependent elasticity and the effect of smectic layering on the defects which has a strong influence on the pairwise colloidal interaction. Finally, we discuss the evolution of loop defects across a photo-induced transition from the cholesteric (N^*) to N. This review is based mainly on the results obtained in our laboratory and also some results of other groups. In this review, we discuss the present state of the experiments and try to give a perspective of how this field could advance in the future.

The manipulation of particles by laser tweezers in LCs is treated as a special case, which contradicts one of the basic requirements, namely, the refractive index of

the particle should be greater than that of the medium. Musevic *et al.* explained different mechanisms behind the trapping and manipulation of colloids with lower refractive index [32]. When the laser power is lower than the optical Fredericksz transition, the surface-induced distortion of the birefringent medium surrounding the particle creates a region of enhanced refractive index for a given polarisation of the laser beam. Hence, the particle behaves effectively as a high-index particle and thus meet the requirement of stable trap. The second trapping mechanism is the creation of a ‘ghost’ particle by optically induced elastic distortion or local decrease (or even melting) of the order parameter of the liquid crystals [32,33]. Figure 2 shows the trapping event of a particle in a homeotropic cell by creating a ghost particle. The particles can also be trapped by thermally creating a gradient of order parameter with the help of the laser tweezers. The particle is attracted to towards the region of lower order as the elastic energy of that

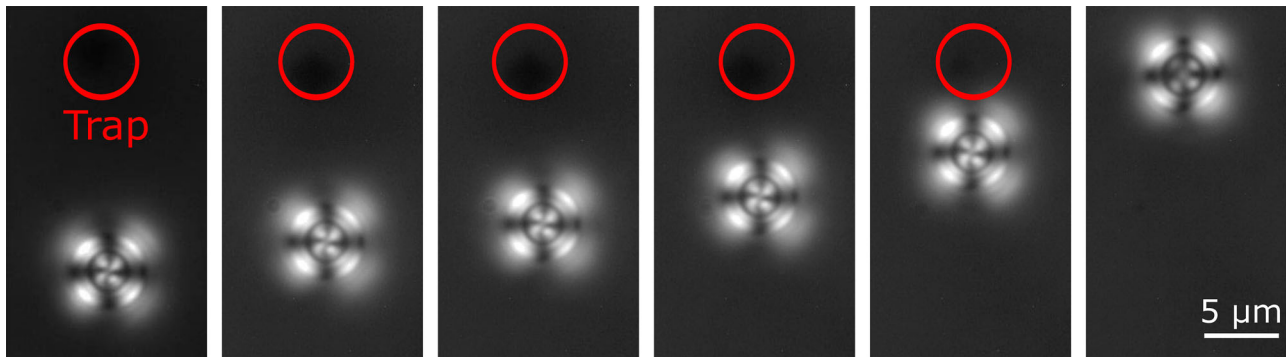


Figure 2. (Colour Online) Laser trapping of a particle in a indium-tin-oxide (ITO) coated homeotropic cell filled with 5CB LC. Particle diameter: $5.2 \mu\text{m}$. Red circles represent laser trapping sites.

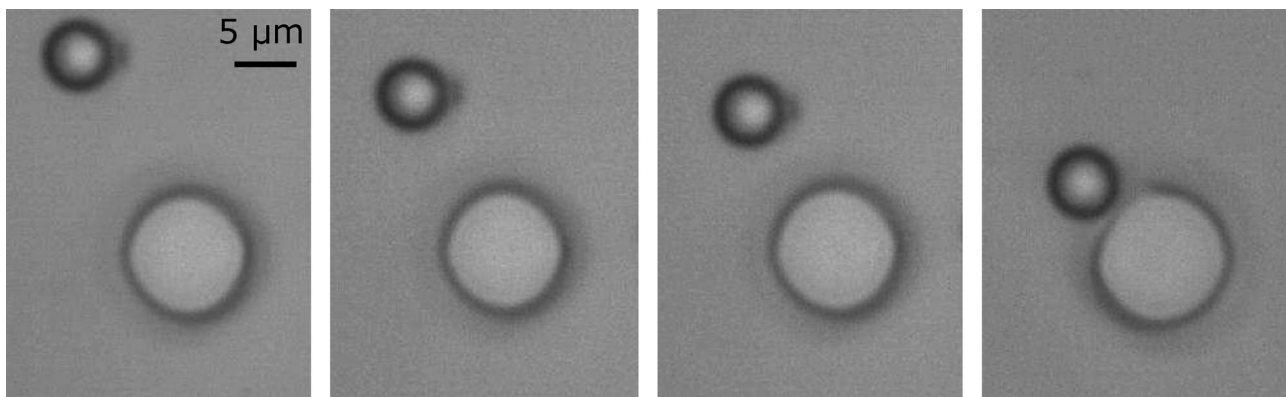


Figure 3. Laser trapping of a dipolar particle in 5CB LC in indium-tin-oxide coated (ITO) planar cell. The laser heating melts the sample locally creating isotropic bubble (big circles).

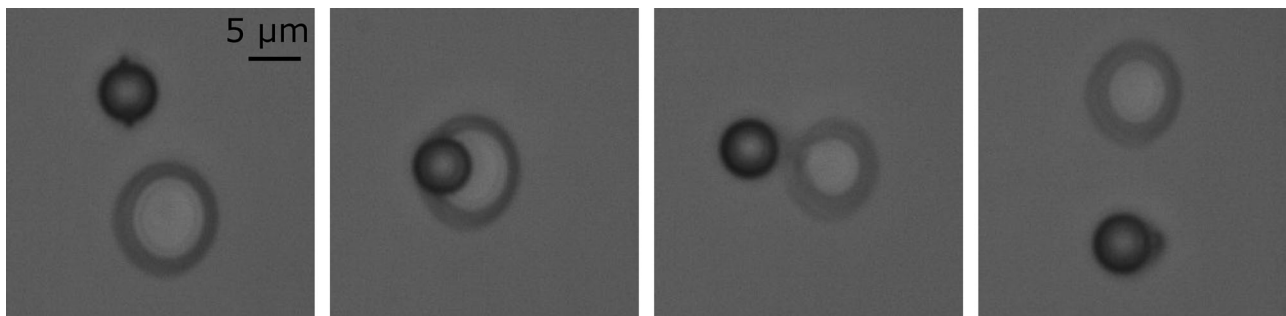


Figure 4. Conversion from a quadrupolar to dipolar particle in 5CB LC using the laser tweezer in a ITO coated planar cell. This transformation is possible in cells with a critical thickness where the gap is comparable to twice the diameter of the particles.

region is lower [34]. Figure 3 shows a trapping event at large laser power in a planar cell made of indium-tin-oxide (ITO) coated glass plates. The laser light creates an isotropic bubble which pulls the particle allowing manipulation at will. The laser tweezers setup is also useful in converting a quadrupolar particle to dipolar particle and vice versa as shown in Figure 4. In this case, the laser light is used to melt the surrounding medium and the defect rewires the particle when the light is switched off.

1.1. Effect of N-SmA transition on dipolar colloids

We begin with the discussion on the effect of N-SmA phase transition on dipolar colloids. Zuhail *et al.* have studied the evolution of elastic dipoles across the N to SmA phase transition [35]. Figure 5(a,c,e) shows three different stages of the evolution of the defect accompanied by a particle across the N-SmA phase transition in a planar cell of 4'-n-octyl-4-cyano-biphenyl (8CB) liquid crystal. As the temperature is reduced, the point defect

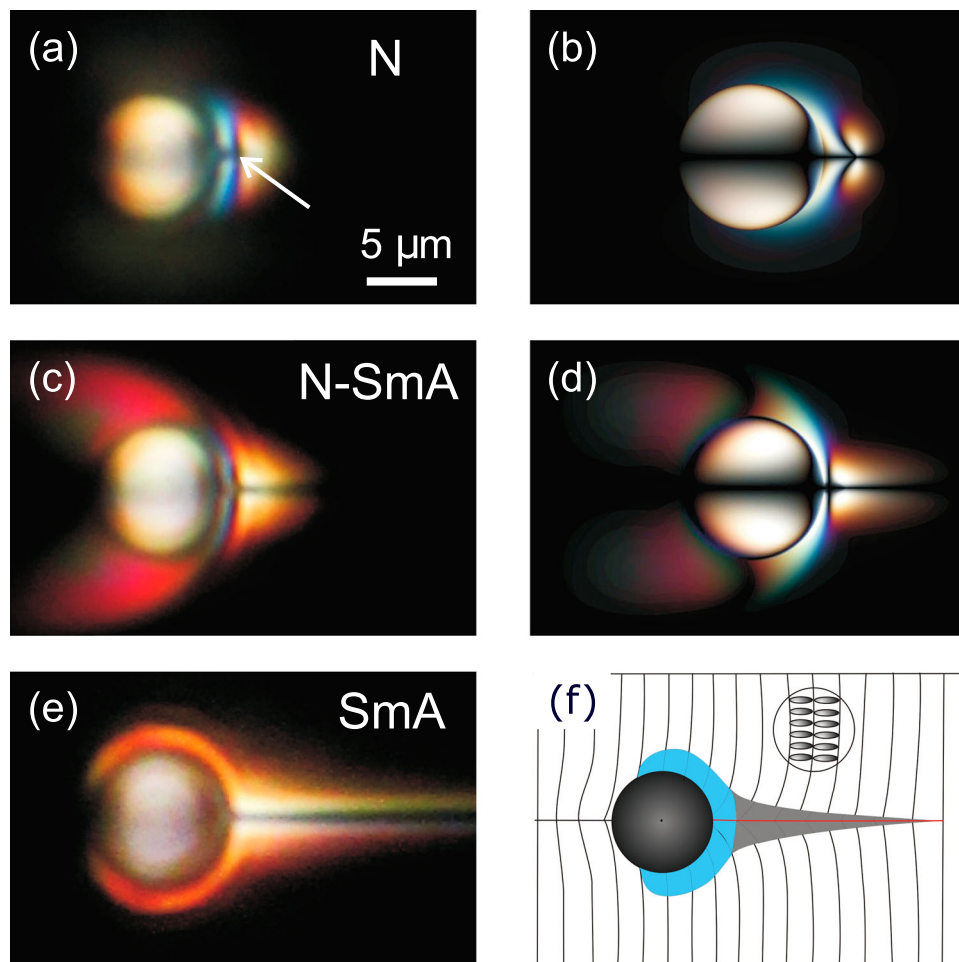


Figure 5. (Colour Online) (a,c,e) Polarising optical photomicrographs of a dipolar particle across the nematic to SmA phase transition in 8CB LC. (a) Just before the N-SmA transition (c) at the transition and (e) after the transition. (b,d) Simulated micrographs in the N phase for (b) equal Frank elastic constants, namely $K_{33} = K_{11}$ and for (d) increased bend elastic constant ($K_{33} = 8K_{11}$). (f) The sketch of layer deformation in the SmA phase is based on the λ -plate image observed in Figure 6(c). Reproduced with permission from [35].

near the particle is forced to move towards the surface and eventually disappears at the surface and a high contrast tail is originated from the same point (compare Figures 5(a) and (e)). The overall texture of the SmA colloid is distinctly different than that of the nematic colloid. It is apparent that the textural change is linked to the change of the relevant elastic constants with temperature. In particular, the bend elastic constant (K_{33}) tends to diverge as the N-SmA transition is approached as a result the bend-splay anisotropy ($\Delta K = K_{33} - K_{11}$) increases rapidly. This significantly increases the bend stress, consequently the director is compelled to rearrange to relax the stress into splay and thereby creating a sort of 'splay soliton' which extends along the rubbing direction.

In the SmA phase, the pre-existing nematic order creates a geometrical constrain on the peripheral region of the particle for the requirement of equally spaced smectic layers. Consequently, the tail is converted to a focal line with discontinuity in the layer orientation

angle that falls off slowly with the distance from the particle (Figure 5(e,f)). The full-wave plate or λ -plate (530 nm) images provide a direct evidence of this effect (Figure 6(a-c)). The magenta colour corresponds to a horizontal orientation of the director, whereas the bluish and yellowish colours correspond to clockwise and anti-clockwise rotation of the director from the rubbing direction, respectively. Thus the director is rotated clockwise above and anti-clockwise below the colloid in the N phase as well as in the SmA phase. Based on this analysis, a schematic representation of SmA layers across the focal line is presented in Figure 5(f). The presmectic evolution of the hyperbolic hedgehog defect was investigated by Landau-de Gennes Q-tensor modelling in the N phase [36]. Figures 5(b,d) show simulated optical transmission micrographs for two elastic constant ratios, namely, $K_{33}/K_{11} = 1$ and $K_{33}/K_{11} = 8$ in the N phase. These ratios correspond to the temperatures far away and very close to the N-SmA transition, respectively. The

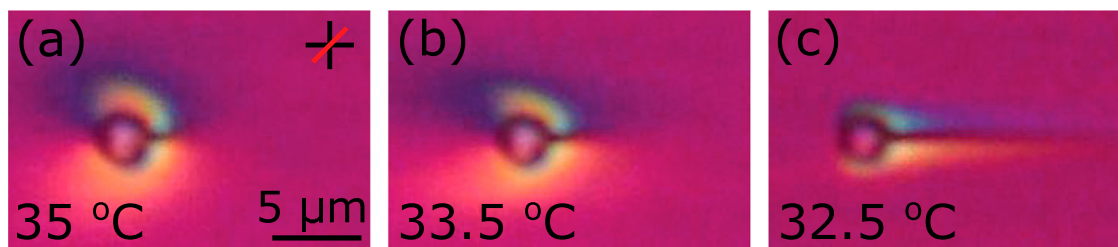


Figure 6. (Colour Online) Optical photomicrographs of a dipolar particle with a λ -plate inserted between the analyser and the sample across the N to SmA phase transition in 8CB LC. (a) In the N phase, (b) at the N-SmA transition and (c) in the SmA phase. Small particle with diameter $2.3 \mu\text{m}$ is chosen to avoid second-order retardation effect.

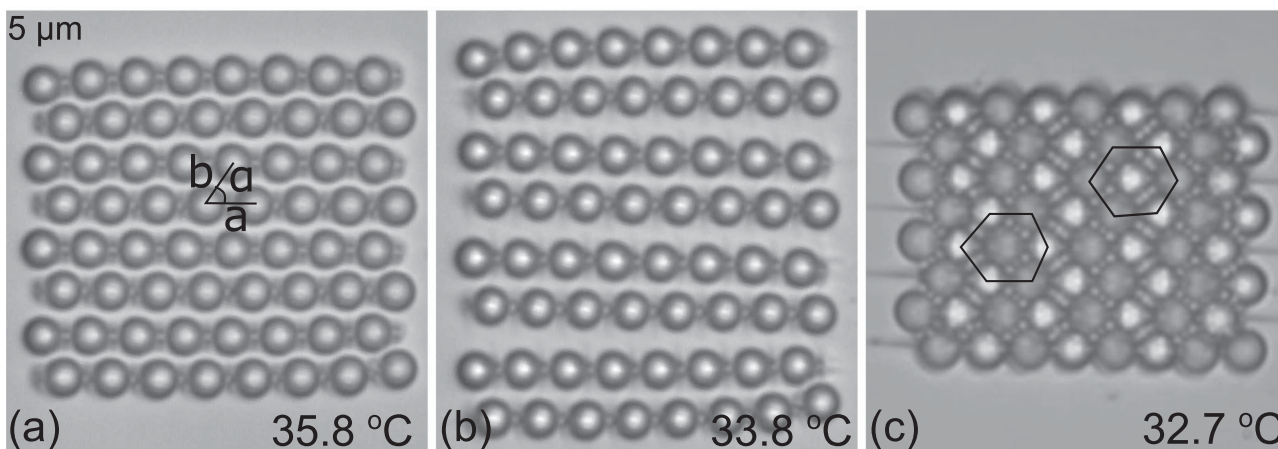


Figure 7. Structural transition of 2D dipolar colloidal crystal across the N-SmA phase transition in 8CB liquid crystal. (a) In the N phase, (b) at the transition, (c) in the SmA phase. Reproduced with permission from [35].

simulated images qualitatively reproduce the experimental results in the nematic phase. A theory or simulation involving the relevant elastic constants of the N and SmA phases will be useful to shed light on the minute details of the transformation.

The dipolar particles have a natural tendency to form linear chains along the director. Such assembly can also be created with the help of laser tweezers. Chains with antiparallel configuration were assembled with the help of the laser tweezers to create a small two-dimensional (2D) colloidal crystal. Figure 7(a) shows a 2D crystal with oblique lattice. The crystal is made of 64 particles of diameter $5.2 \mu\text{m}$ in a planar cell. The stability of the structure is obtained by balancing the long-range attractive elastic forces with the short-range repulsive force. The latter force arises due to the point defects between the particles. An interesting effect was observed when the sample was cooled across the N-SmA phase transition. Figure 7 shows a sequence of bright field images of the dipolar crystal across the N-SmA phase transition. Near the transition temperature, the crystal tends to expand in a direction perpendicular to the chains (Figure 7(b)). The point defects disappear at the transition. The disappearance of the defects causes the collapse of the crystal into

a hexagonal structure in the SmA phase (Figure 7(c)). This effect is reversible across the phase transition. Thus the colloidal crystals can be restructured from oblique to hexagonal by going through the N to SmA phase transition.

1.2. Effect of N-SmA transition on quadrupolar colloids

Particles with homeotropic surface anchoring also stabilises elastic quadrupoles (dressed with Saturn ring) [38] below a critical ratio of the diameter and the thickness of the cell [39]. Zuhail *et al.* studied the effect of N-SmA phase transition on quadrupolar colloids [37]. Figure 8(a–d) shows a few snapshots of a quadrupolar particle across the phase transition. In the N phase, four lobes with birefringent colour are observed. It shows distortion around the particle which are extending as the N-SmA transition point is approached (Figure 8(b)). The lobes shrink to a narrow region showing a ring type appearance on the surface of the particle just below the N-SmA transition temperature (Figure 8(c)). The ring almost disappears and two horizontal faint bands appear at further reduced temperature in the SmA phase

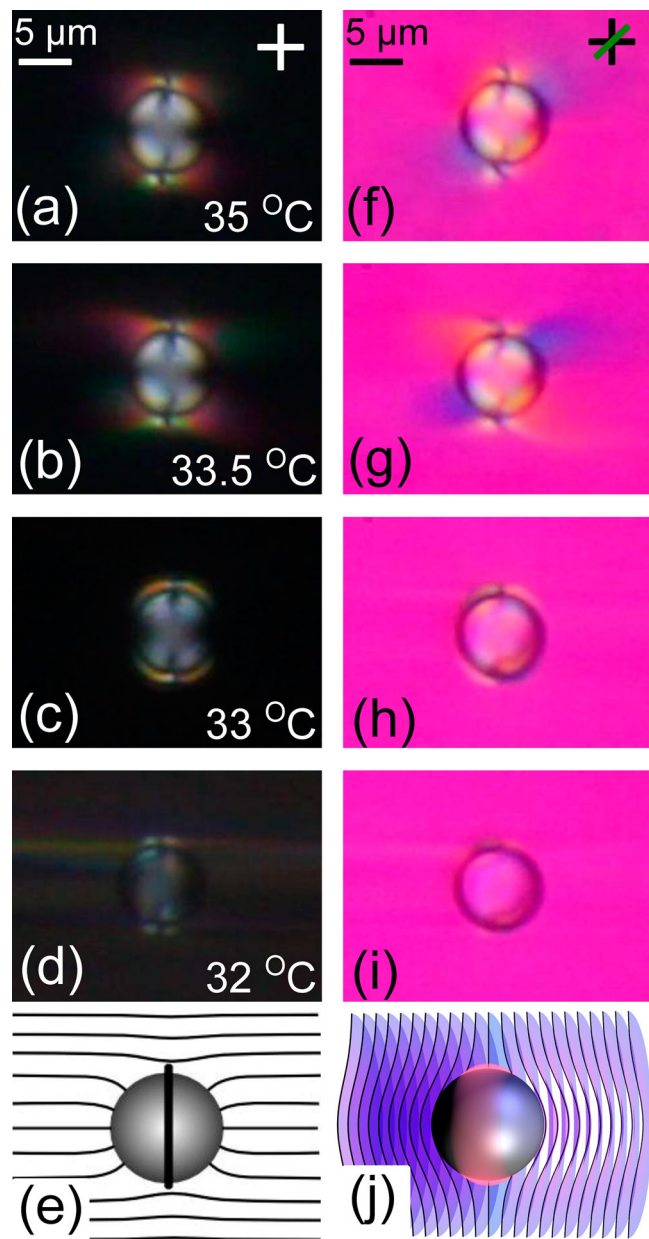


Figure 8. (Colour Online) (a)–(d) Polarising optical photomicrographs of a quadrupolar particle in 8CB across the N-SmA phase transition. (f–i) Corresponding images with the red wave-plate (green line denotes the slow axis). Schematic representation of the (e) director above the transition (j) SmA layers. Reproduced with permission from [37].

(Figure 8(d)). Figure 8(f–i) shows the corresponding λ -plate images. The anchoring of the director on the surface of the particle in the SmA phase is broken. Monte Carlo simulation by Schlotthauer et al. also supports this observation [40]. They showed that the effective anchoring decreases as the nematic to SmA transition is approached. They performed simulation with different anchoring strength and computed local density and nematic order parameter. In strong surface anchoring regime, the ring defect does not vanish in the SmA phase

as observed in the experiment. In case of weaker surface anchoring, the colloid is unable to bend the smectic layers around its equator and therefore the smectic layers remain almost equidistant in the vicinity of the particle. Consequently, no defects are formed [40]. Based on the λ -plate images as shown in Figure 8(h–i), a schematic representation of approximate layer orientation in the SmA phase is shown in Figure 8(j). The pre-smectic evolution of defect is originated from the temperature dependent bend-splay elastic anisotropy which is confirmed by numerical simulation using Landau-de-Gennes Q-tensor modelling. Figure 9(a–c) shows the experimental textural changes of a pair of quadrupolar colloids at different temperatures as the N-SmA temperature is approached. As this transition is approached, the ratio of K_{33}/K_{11} increases. Figure 9(d–f) shows simulated images at three different ratios of K_{33}/K_{11} which agrees reasonably well with the experimentally observed textures at different temperatures.

Such particles usually stabilise straight or kinked chains in uniform NLCs which can be directed by the laser tweezer for assembling 2D colloidal crystals as shown in Figure 10(a). It shows an oblique lattice in the nematic phase. When the temperature is reduced across the N-SmA phase transition, the crystal structure tends to expand along the rubbing direction (Figure 10(b)) and then in the SmA phase, it breaks apart into chains of different lengths (Figure 10(c)). This transition is irreversible compared to the reversible transition in dipolar crystals. This is expected as the quadrupolar crystals are unstable due to much weaker binding energy per particle than the dipolar crystals.

1.3. Effect of N-SmA transition on boojum colloids

When the particles with planar surface anchoring are dispersed into an NLC, two antipodal defects known as boojums are induced (see Figure 1(i)). They are a pair of surface defects on the poles of the particle along the far field director. There are a very few theoretical and experimental studies on the effect of phase transition on boojum colloids and their interactions [13–16].

Blanc and Kleman have studied microdroplets of glycerine in an aligned smectic phase of 8CB. They observed that the spherical droplets provide planar anchoring to SmA layers and induce two singular line defects extending along the director (Figure 11(a,b)) [41]. They calculated the curvature energy and showed that the angular discontinuity of layers decreases continuously far from the droplet interface. Based on the calculations, they proposed schematic diagrams showing deformation of SmA layers for various radii of the microdroplets (Figure 11(c)).

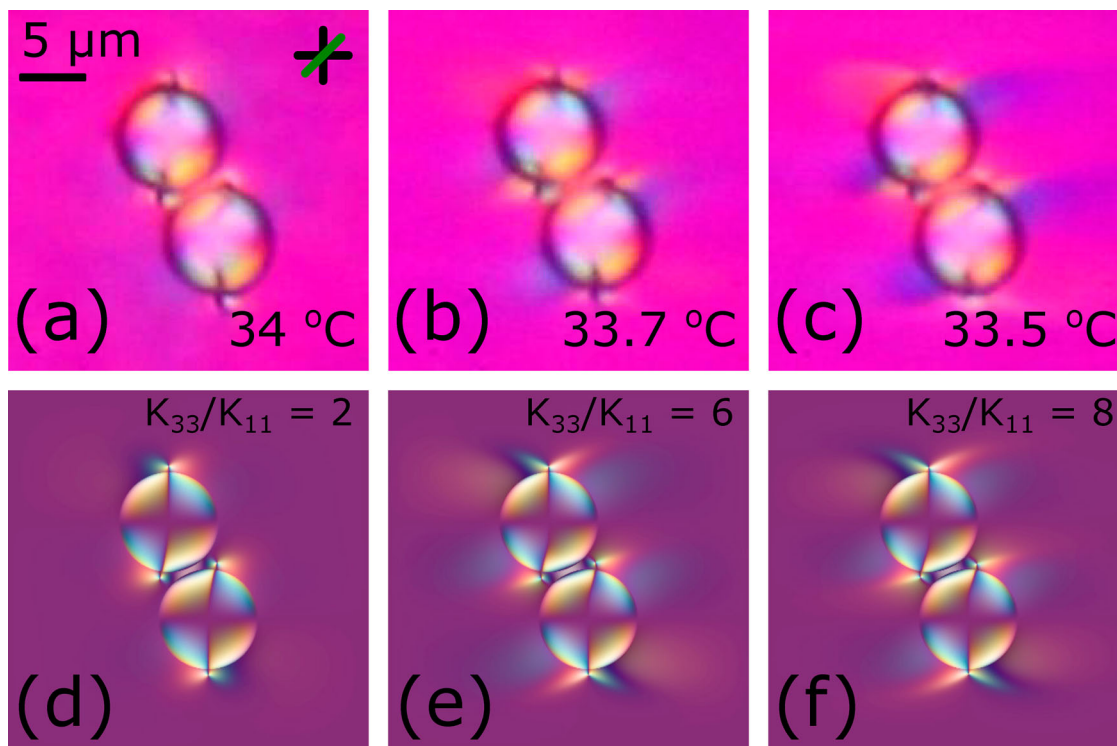


Figure 9. (Colour Online) (a-c) Optical photomicrographs taken with with red wave-plate just before the N-SmA phase transition of a pair of quadrupolar particles in 8CB. (d-f) Simulated images with the λ -plate at various ratios of K_{33}/K_{11} . Reproduced with permission from [37].

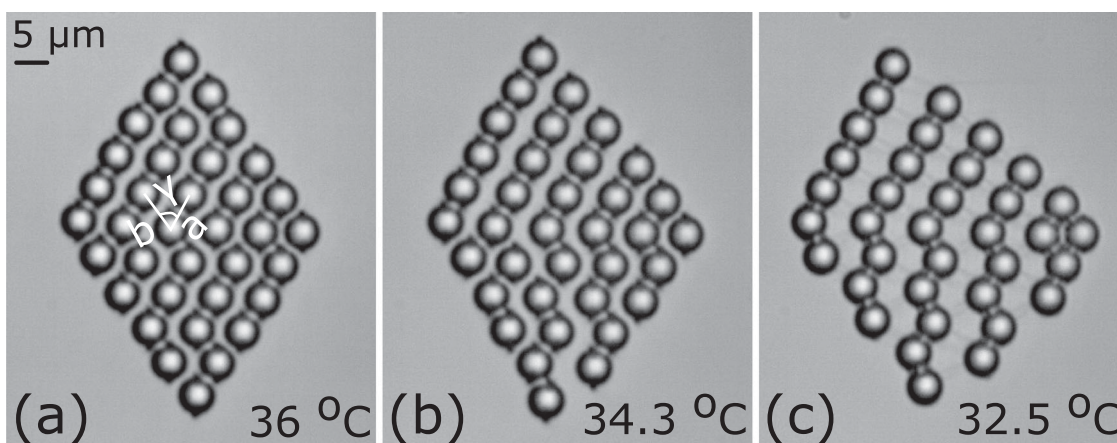


Figure 10. Bright field optical photomicrographs showing the structural change of 2D quadrupolar crystal across the N-SmA transition in 8CB LC. Particle size is $5.2 \mu\text{m}$ and cell thickness is $8 \mu\text{m}$. Reproduced with permission from [37].

Zuhail *et al.* studied the effect of N-SmA phase transition on boojum colloids [42]. The colloids are treated with N-Trimethoxysilylpropyl- N,N,N-trimethylammonium chloride (MAP) for planar anchoring. Figures 12(a-c) show the polarising optical microscope images of a boojum particle and the transformation of the defects across the N-SmA phase transition in 8CB LC. The elastic distortion increases along the rubbing direction as the N-SmA transition is approached (Figure 12(b)). In the SmA phase, the distortion is further

extended and a high contrast tail with a straight dark-line on both poles of the particle along the rubbing direction is observed. This is somewhat similar to the focal line that was observed in the case of hyperbolic hedgehog defect in dipolar particles across the N-SmA transition (Figure 5(e)). One important difference is that, the point defect moves toward the surface of the dipolar particle just before the transition, whereas similar movement is not observed in the case of boojum colloid as the points are always residing on the surface of

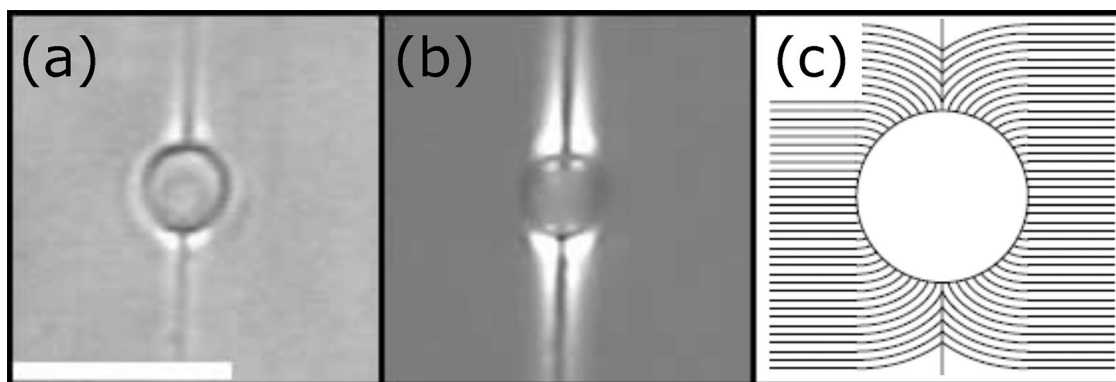


Figure 11. Optical photomicrographs of a droplet of glycerine in SmA phase of 8CB LC (a) without and (b) with crossed polarisers. (c) Schematic representation of layer deformation in the vicinity of the droplet. Reproduced with permission from [41].

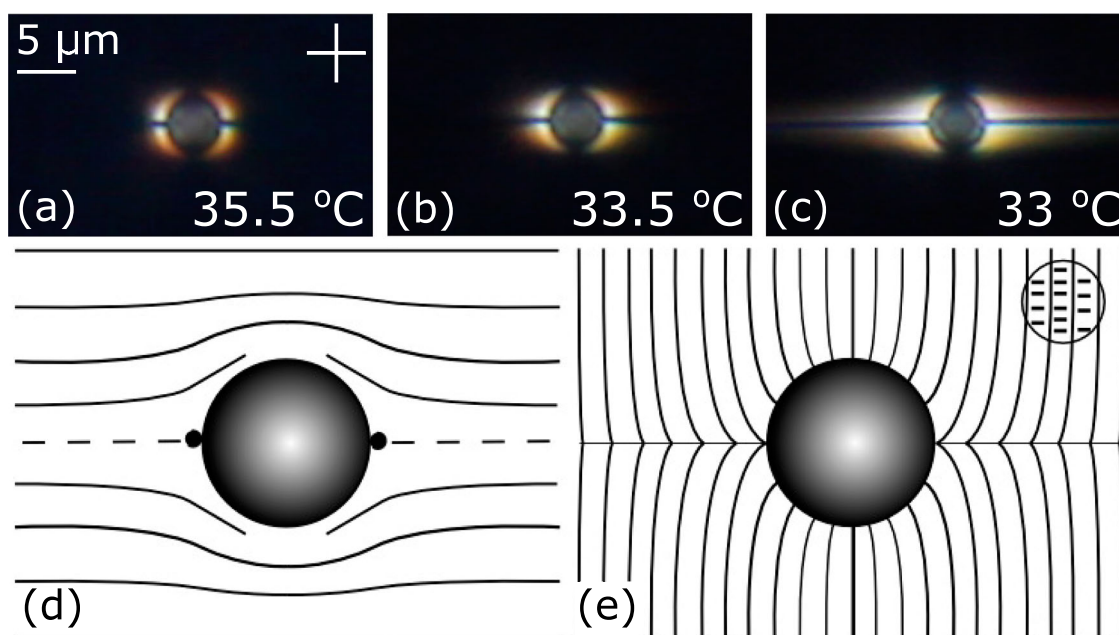


Figure 12. (Colour Online) Polarising optical photomicrographs of a boojum colloid in a planar cell (a) in the N phase, (b) at the N-SmA phase transition and (c) in the SmA phase of 8CB LC. Schematic diagram of (d) the nematic director orientation around the particle (e) the SmA layers in the vicinity of the particle with focal conic line defects. Reproduced with permission from [42].

the particle. The brighter regions in the neighbourhood of the particle in the SmA phase indicate that the layers are strongly bent. For investigating the molecular orientation around the particle, a low birefringence LC (CCN-47, $\Delta n = 0.03$) was chosen for analysing λ -plate images. In such samples, the second-order retardation effect due to increased birefringence of the SmA phase is easily avoided. It exhibits N-SmA phase transition at 28.2°C . Figure 13 shows some snapshots across the N-SmA phase transition. The bluish and yellowish colours correspond to the clockwise and anti-clockwise rotation of the director from the rubbing direction as mentioned previously. By comparing Figure 13(a–c), a schematic representations of LC director around the particle in the N and SmA phases (with focal conic lines) are shown in Figure 12(d,e), respectively. These focal conic lines

are parallel to the rubbing direction, being less and less visible far from the microsphere. In the simulation, when the surface anchoring is weak, two point-like defects are observed in the SmA phase [40]. At high anchoring strength, the defects in the SmA phase spread over a large range and look similar to focal conic lines. Here the focal lines are formed due to the angular discontinuity of the SmA layer orientation.

Boojum colloids tend to form linear chains spontaneously. Usually are aligned at an angle 30° with respect to the far-field director. These chains are directed to assemble using laser tweezers and a small 2D crystal is prepared in the N phase. When the temperature is decreased across the N-SmA phase, these defects disappear at the transition and the restructuring of the colloids takes place. Figure 14 shows a sequence of images

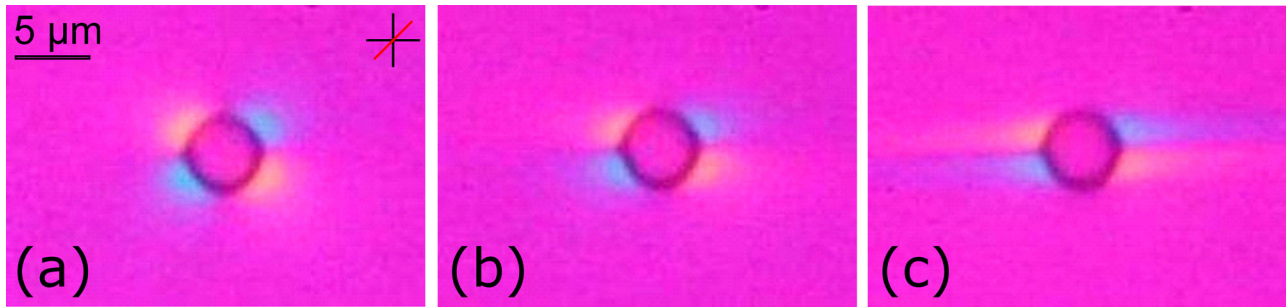


Figure 13. (Colour Online) Optical photomicrograph of a boojum particle with a λ -plate across the N to SmA phase transition in CCN-47 LC. (a) In the N phase, (b) at the N-SmA transition and (c) in the SmA phase.

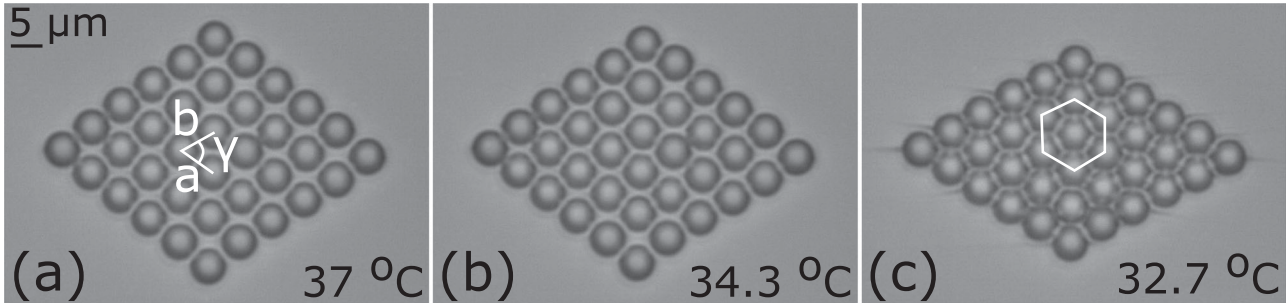


Figure 14. Bright field images showing a structural change in 2D boojum crystal across the N-SmA transition in 8CB LC. (a) N phase (b) at the N-SmA transition (c) SmA phase. Reproduced with permission from [42].

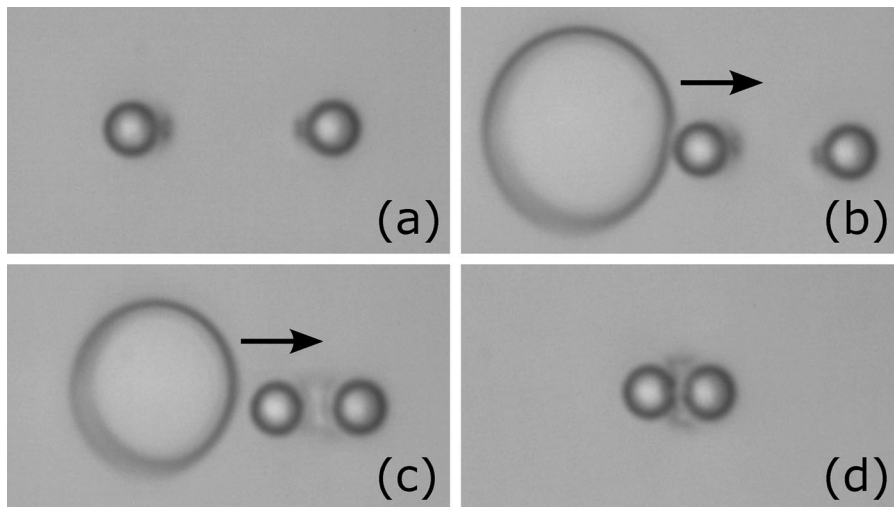


Figure 15. (a–d) Sequence of images showing the formation of vortex-like defect by pushing two repelling dipolar particles using laser tweezers in a ITO coated planar cell of 5CB LC. Arrows indicate the pushing direction. Big circles are isotropic bubble created by the laser beam. Silica particle diameter: 5.2 μm .

representing the structural changes of 2D colloidal crystal with boojum defects across the N-SmA phase transition. The unit cell changes from the oblique in the N phase to hexagonal close pack in the SmA phase.

1.4. Effect of N-SmA transition on colloids with vortex-like defect

In what follows we discuss the effect of phase transitions on nonsingular defects. Usually in planar cells two

collinear and parallel dipoles are attracted to each other whereas the antiparallel dipoles are repelled. However, if two anti-parallel dipoles are pushed together against their elastic repulsion using the laser tweezers as illustrated in Figure 15(a–d), it forms an escaped non-singular vortex-like defect of strength -2 , which is also popularly known as the ‘bubblegum defect’ [43–46]. Basically it forms a kind of elastically bonded dimer. Zuhail et al. studied the transformation of such particles across the N to SmA phase transition [47]. Figure 16(a) shows a dimer

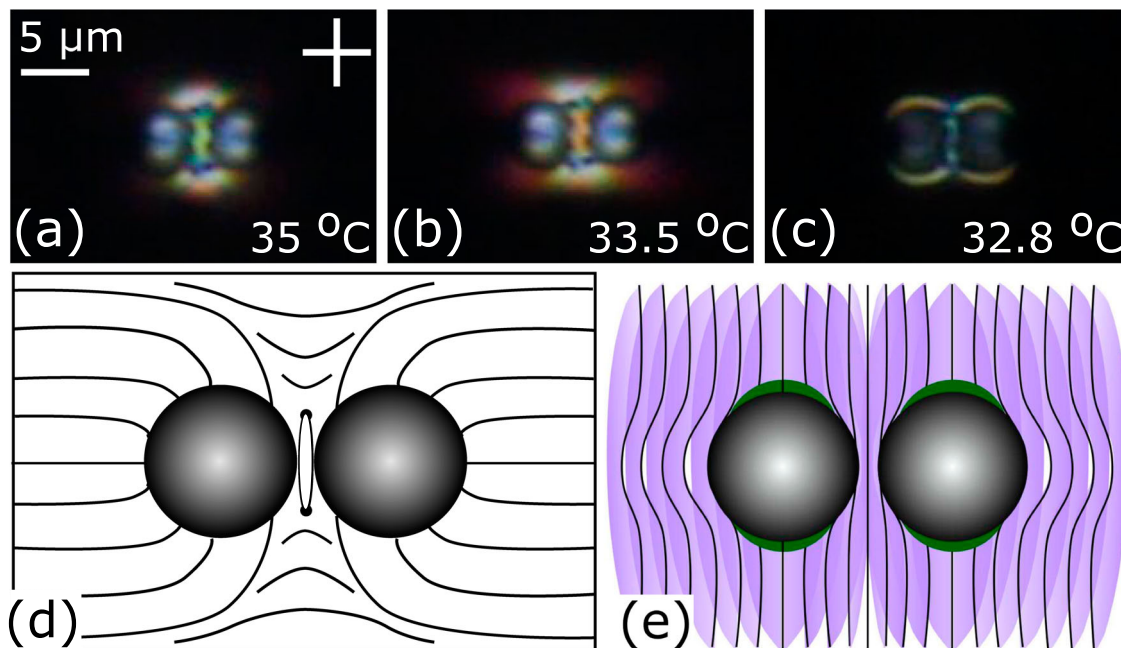


Figure 16. (Colour Online) Polarising optical micrographs of a dimer with vortex-like defect across the N-SmA transition in 8CB LC. A dimer (a) in the N phase, (b) at the N-SmA phase transition and (c) in the SmA phase. Schematic diagram of (d) the director orientation in the N phase and (e) the SmA layer deformation surrounding the particle. The green colour indicates the regions where the homeotropic anchoring is broken and the layer orientation can not be discerned clearly. Reproduced with permission from [47].

formed by pushing two collinear antiparallel dipoles with a laser tweezer in the nematic phase of 8CB liquid crystal. The complex distortion of local director field between the colloids is clearly observed in the POM micrographs (Figure 16(a)). It has been reported that the director field around the bubblegum is axially symmetric, minimally distorted and continuous as shown schematically in Figure 16(d). As the temperature is reduced towards the N-SmA transition, the director distortion between the colloids and in their surrounding tends to enhance (Figure 16(b)). Below the transition, the deformation shrinks to a narrow ring-like regions around the particles (Figure 16(c)) and the interparticle distance is reduced compared to the N phase.

To get a qualitative idea about the layer deformation in the SmA phase, a low birefringent liquid crystal (CCN-47) was used for analysing λ -plate images. Figure 17 shows the image of a dimer across the N-SmA phase transition with a λ -plate. As mentioned previously, the magenta colour corresponds to a horizontal orientation of the director, whereas bluish and yellowish colours correspond to clockwise and anti-clockwise rotation of the director from the rubbing direction, respectively (Figure 17(a–b)). In the SmA phase the narrow region between the two particles looks uniformly magenta colour, indicating the layer are uniform. In addition, surrounding the particles, a ring-like highly confined region with opposite colours are observed (Figure 17(c)).

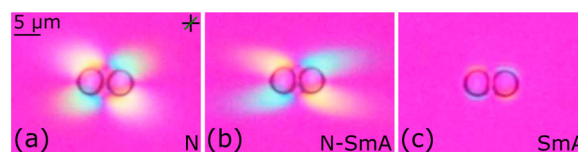


Figure 17. (Colour Online) Optical micrograph of a dimer with the λ -plate across the N-SmA transition in CCN-47 LC. A dimer in (a) the N phase, (b) at the N-SmA phase transition and (c) in the SmA phase. Green line denotes the slow axis. Reproduced with permission from [47].

By analysing the far field region, the far field smectic layer structure of the dimer is depicted schematically in Figure 16(e). In the confined region the homeotropic anchoring is broken and the director appears to be tilted in opposite direction creating a complex layer deformation which can not be discerned easily (see green colour region in Figure 16(e)). Figure 18 presents a sequence of images showing a structural change of 2D colloidal crystal across the N-SmA transition in 8CB liquid crystal. It shows an oblique lattice. The lattice constants are reduced nearly by 35% in the SmA phase compared to that of the N-phase.

1.5. Effect of SmA-SmC transition on dipolar colloids

There are several studies on the colloidal dispersion in smectic free standing films [48–51] and at the SmA-air

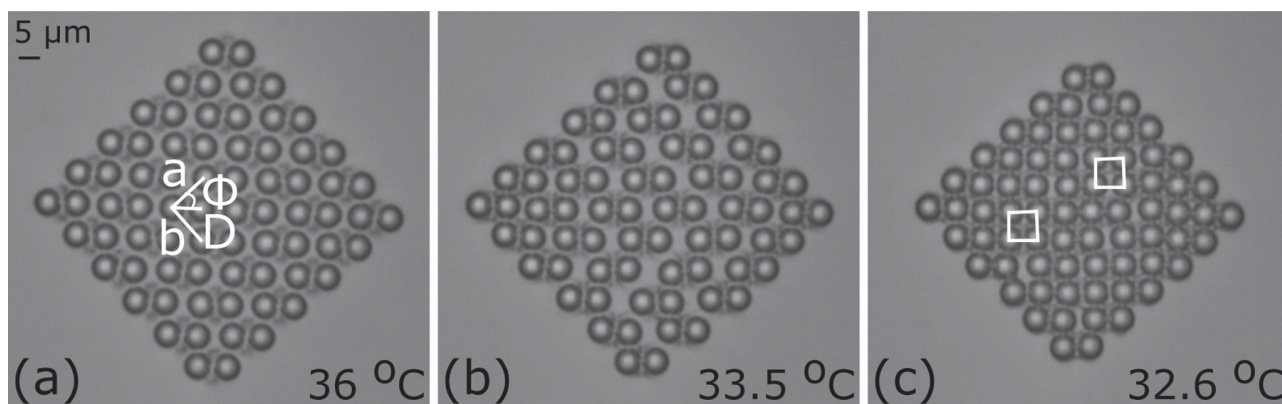


Figure 18. Bright field images (without crossed polarisers) showing the structural transition of 2D colloidal crystal (with vortex-like defects) across the N-SmA phase transition in 8CB LC. (a) N phase (b) at the N-SmA transition (c) SmA phase. Reproduced with permission from [47].

interface [52] but the number of experimental and theoretical studies are meagre on bulk systems although some interesting effects has been predicted theoretically [39,53–57]. For example, Santangelo *et al.* theoretically predicted that the nonlinear elasticity of the SmA due to spherical inclusion could give rise to an attractive interaction [54]. Tovkach *et al.* calculated the interaction of small particles in SmA LCs and predicted that the elastic distortion induced interaction is oscillatory and can give rise to superstructures with finite interparticle distance [55]. Most of these predictions are far from experimental verification. From the experimental point of view, the main problem is that the particles are expelled from the medium due to the one-dimensional positional order and the large layer compression modulus of smectic liquid crystals.

Patricio *et al.* calculated the effective interaction between two circular disks immersed in smectic-C films mediated by the topological defects using a two-dimensional elastic-free energy [51]. They reported that for a large disk separations (D), the elastic-free energy scales as $\approx D^{-2}$, which confirms the dipolar character of the long-range effective interaction. Colloidal inclusions and formation of chains and clusters in oriented smectic membranes have also been investigated experimentally [49] and numerically [59]. Studies show that the shape of small droplets embedded in smectic membranes differ considerably from circular form to minimise the free energy [60,61]. They observed elliptical, elongated circles and spindle like shapes along with circular shape. Muhammed *et al.* studied a pair of microparticles with homeotropic and planar surface anchoring across N-SmA-SmC phase transitions [58]. Figure 19(a–c) shows morphological changes of a pair of dipolar particles across the N-SmA-SmC phase transitions. Some snapshots taken at different phases with λ -plate are also

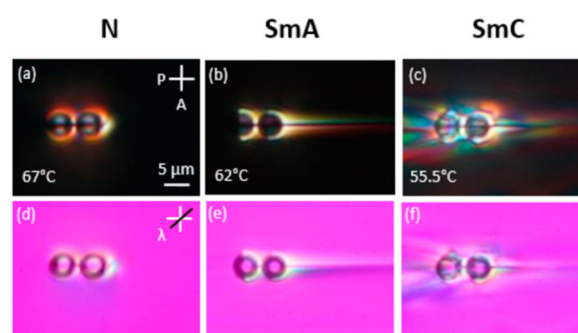


Figure 19. (Colour Online) Optical photomicrographs of a pair of collinear dipolar particles across the N-SmA-SmC transitions. Images are taken (a–c) with crossed polarisers, (d–f) with a λ -plate. Reproduced with permission from [58].

shown in Figure 19(d–f). The transformation of the defect structure across N-SmA transition is similar to that was observed in Figure 5. In the SmC phase the structure, however, becomes very complex. The surface anchoring is mostly broken and the surrounding layer deformation becomes highly nonuniform (Figure 19(c)) [58].

1.6. Effect of N-N* transition on quadrupolar colloids

There are some experimental and theoretical studies on the topological defects induced by spherical particles in cholesteric (N*) liquid crystals. It has been reported that the structure of the defects and interaction depends on the relative size (R) of the particle and the helical pitch P . For example, when $R \ll P$, the particles experience homogeneous nematic order and creates elastic dipoles or quadrupoles. However, by shortening the helical pitch, the point defect or the circular ring defect transforms into a strongly deformed defect loop. Numerical calculations

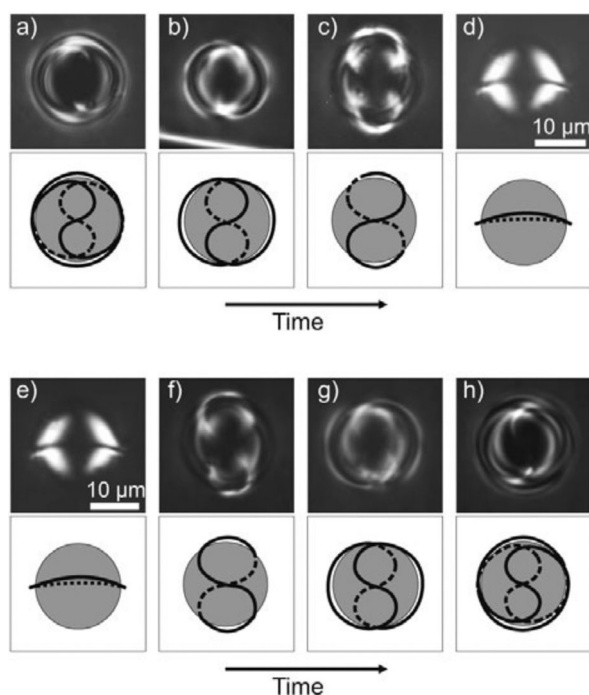


Figure 20. A defect ring is wound around the silica particle with homeotropic surface anchoring in a cell filled with photosensitive chiral mixture (left-handed cholesteric, LHC). Under continuous UV irradiation, the mixture goes from LHC to unwind and then to right-handed cholesteric (RHC). (a–d) Irreversible unwinding from LHC to N. (e–h) Irreversible UV light-induced winding from N to right-handed cholesteric (RHC). Reproduced with permission from [62].

by Lintuvuori *et al.* [63,64] and experimental studies of Senyuk *et al.* [65] showed that, particles with planar surface anchoring in the bulk cholesteric LC are decorated by defect loops. When R/P increases, a twisted set of disclination lines of opposite chirality wraps the particle. Jampani *et al.* systematically studied the defect structures and entanglement of colloidal dimers in twisted cells. They observed various entangled defect structures depending upon the twist angle [66]. Gvozdevskyy *et al.* studied the winding and unwinding of Saturn ring defects around silica microspheres with homeotropic surface anchoring in a cholesteric LC with a variable pitch (see Figure 20) [62]. They used mixtures of 5CB liquid crystal and various photoresponsive chiral dopants to vary the helical pitch by illuminating the mixtures with UV or visible light. With increasing exposure time the helix changes from left-handed cholesteric (LHC) to nematic (N) and then to right-handed cholesteric (RHC) irreversibly. In particular, under UV irradiation, the cholesteric helix is gradually unwound from the initial 3π winding across the particle (Figure 20(a)) to 2π winding (Figure 20(b)) and then to π winding (Figure 20(c)). The defect loop in the π -structure is comparatively less twisted and a ‘figure

of eight’ loop is clearly seen. Upon further irradiation, the defect loop unwinds irreversibly from LHC to N and forms a Saturn ring (Figure 20(d)). With increasing exposure time, the system went from N to RHC, consequently, (Figure 20(e–h)).

2. Conclusion

We have presented a brief overview on the recent developments on the particle induced defect morphogenesis across the phase transitions of liquid crystals. We have mostly discussed the dipolar, quadrupolar and boojum-colloids and their transformation across the phase transition to SmA, SmC or cholesteric phases. Uniform surface anchoring of the LC director on the particles is broken in the SmA or SmC phases. As a result a strong deformation of layers are observed surrounding the particles along with focal conic lines. The defects associated with the particles disappear at the N-SmA phase transition. The pretransitional divergence of bend elastic constant across the N-SmA transition is responsible for resulting deformation and defect structure in the SmA phase. The phase transition also has a strong influence on the colloidal pair interaction and is responsible for the structural transition of 2D colloidal assemblies. Studies so far have focused on spherical particles with homeotropic or planar surface anchoring, but a plethora of new particles with controlled shape and anchoring available [67–70], promise a wide range of interesting effects. A theory or simulation involving the relevant elastic constants of the phases which could provide insights into the evolution of the defect structure across phase transitions is naturally a theoretical challenge.

Acknowledgments

This work is supported by the DST, Govt. of India (DST/SJF/PSA-02/2014-2015) and Slovenian Research Agency (ARRS) (P1-0099, N1-0104, N1-0116). S. D. acknowledges a Swarnajayanti Fellowship.

Disclosure statement

No potential conflict of interest was reported by the authors.

Funding

This work is supported by the Department of Science and Technology (DST), Govt. of India [grant number DST/SJF/PSA-02/2014-2015] and Slovenian Research Agency (ARRS) [grant numbers P1-0099, N1-0104, N1-0116].

ORCID

Matjaž Humar  <http://orcid.org/0000-0003-3338-6723>
Surajit Dhara  <http://orcid.org/0000-0003-3144-0300>

References

- [1] de Gennes PG, Prost J. The physics of liquid crystals. 1995. (International Series of Monographs on Physics).
- [2] Chandrasekhar S. Liquid crystals. 2nd ed. Cambridge (UK): Cambridge University Press; 1992.
- [3] Bahr C, Kitznerow HS. Chirality in liquid crystals. Heidelberg: Springer; 2001.
- [4] Poulin P, Stark H, Lubensky TC, et al. Novel colloidal interactions in anisotropic fluids. *Science*. 1997;275:1770–1773.
- [5] Mušević I. Liquid crystal colloids. 2017. (Springer International Publishing AG).
- [6] Smalyukh II. Liquid crystal colloids. *Annu Rev Condens Matter Phys*. 2018;9:207–216.
- [7] Mušević I, Škarabot M, Tkalec U, et al. Two-dimensional nematic colloidal crystals self-assembled by topological defects. *Science*. 2006;313:954–958.
- [8] Stark H. Physics of colloidal dispersions in nematic liquid crystals. *Phys Rep*. 2001;351:387–474.
- [9] Trivedi RP, Engstrom D, Smalyukh II. Optical manipulation of colloids and defect structures in anisotropic liquid crystal fluids. *J Opt*. 2011;13:044001.
- [10] Kuksenok OV, Ruhwandl RW, Shiyanovskii SV, et al. Director structure around a colloid particle suspended in a nematic liquid crystal. *Phys Rev E*. 1996;54:5198.
- [11] Poulin P, Cabuil V, Weitz DA. Direct measurement of colloidal forces in an anisotropic solvent. *Phys Rev Lett*. 1997;79:4862.
- [12] Mozaffari MR, Babadi M, Fukuda JI, et al. Interaction of spherical colloidal particles in nematic media with degenerate planar anchoring. *Soft Matter*. 2011;7:1107–1113.
- [13] Eskandari Z, Silvestre NM. Bonded boojum-colloids in nematic liquid crystals. *Langmuir*. 2013;29:10360–10367.
- [14] Liu Q, Senyuk B, Tasinkevych M, et al. Nematic liquid crystal boojums with handles on colloidal handlebodies. *Proc Natl Acad Sci USA*. 2013;110:9231–9236.
- [15] Tasinkevych M, Silvestre NM. Liquid crystal boojum-colloids. *New J Phys*. 2012;14:073030.
- [16] Smalyukh II, Lavrentovich OD, Kuzmin AN, et al. Elasticity-mediated self-organization and colloidal interactions of solid spheres with tangential anchoring in a nematic liquid crystal. *Phys Rev Lett*. 2005;95:157801.
- [17] Loudet JC, Poulin P, Barois P. Edge dislocations of colloidal chains suspended in a nematic liquid crystal. *Europhys Lett*. 2001;54:175.
- [18] Nazarenko VG, Nych AB, Lev BI. Crystal structure in nematic emulsion. *Phys Rev Lett*. 2001;87:075504.
- [19] Gu Y, Abbott NL. Observation of Saturn-ring defects around solid microspheres in nematic liquid crystals. *Phys Rev Lett*. 2000;85:4719.
- [20] Lubensky TC, Pettey D, Currier N, et al. Topological defects and interactions in nematic emulsions. *Phys Rev E*. 1998;57:610.
- [21] Petrov PG, Terentjev EM. Formation of cellular solid in liquid crystal colloids. *Langmuir*. 2001;17:2942–2949.
- [22] Yada M, Yamamoto J, Yokoyama H. Direct observation of anisotropic interparticle forces in nematic colloids with optical tweezers. *Phys Rev Lett*. 2004;92:185501.
- [23] Pawsey AC, Clegg PS. Colloidal particles in blue phase liquid crystals. *Soft Matter*. 2015;11:3304.
- [24] Nych A, Ognysta U, Škarabot M, et al. Assembly and control of 3D nematic dipolar colloidal crystals. *Nat Commun*. 2015;4:1289.
- [25] Rasna MV, Zuhail KP, Ramudu UV, et al. Orientation, interaction and laser assisted self-assembly of organic single crystal micro-sheets in nematic liquid crystal. *Soft Matter*. 2015;11:7674.
- [26] Ognysta U, Nych A, Nazarenko V, et al. Design of 2D binary colloidal crystals in a nematic liquid crystal. *Langmuir*. 2009;25:12092–12100.
- [27] Sahu DK, Anjali TG, Basavraj MG, et al. Orientation, elastic interaction and magnetic response of asymmetric colloids in a nematic liquid crystal. *Sci Rep*. 2019;9:1–10.
- [28] Senyuk B, Liu Q, Bililign E, et al. Geometry-guided colloidal interactions and self-tiling of elastic dipoles formed by truncated pyramid particles in liquid crystals. *Phys Rev E*. 2015;91:040501(R).
- [29] Rasi M, Pujala RK, Dhara S. Colloidal analogues of polymer chains, ribbons and 2D crystals employing orientations and interactions of nano-rods dispersed in a nematic liquid crystal. *Sci Rep*. 2019;9:1–11.
- [30] Sudhakaran DV, Pujala RK, Dhara S. Orientation dependent interaction and self-assembly of cubic magnetic colloids in a nematic liquid crystal. *Adv Opt Mater*. 2020;8:1901585.
- [31] Pishnyak OP, Tang S, Kelly JR, et al. Levitation, lift, and bidirectional motion of colloidal particles in an electrically driven nematic liquid crystal. *Phys Rev Lett*. 2007;99:127802.
- [32] Mušević I, Škarabot M, Babič D, et al. Laser trapping of small colloidal particles in a nematic liquid crystal: clouds and ghosts. *Phys Rev Lett*. 2004;93:187801.
- [33] Škarabot M, Ravnik M, Babič D, et al. Laser trapping of low refractive index colloids in a nematic liquid crystal. *Phys Rev E*. 2006;73:021705.
- [34] Škarabot M, Lokar Z, Mušević I. Transport of particles by a thermally induced gradient of the order parameter in nematic liquid crystals. *Phys Rev E*. 2013;87:062501.
- [35] Zuhail KP, Sathyanarayana P, Seč D, et al. Topological defect transformation and structural transition of two-dimensional colloidal crystals across the nematic to smectic-A phase transition. *Phys Rev E*. 2015;91:030501.
- [36] Ravnik M, Žumer S. Landau-de gennes modelling of nematic liquid crystal colloids. *Liq Cryst*. 2009;36:1201–1214.
- [37] Zuhail KP, Čopar S, Mušević I, et al. Spherical microparticles with Saturn ring defects and their self-assembly across the nematic to smectic-A phase transition. *Phys Rev E*. 2015;92:052501.
- [38] Mondain-Monval O, Dedieu JC, Gulik-Krzywicki T, et al. Weak surface energy in nematic dispersions: Saturn ring defects and quadrupolar interactions. *Eur Phys J B*. 1999;12:167–170.
- [39] Ognysta U, Nych A, Nazarenko V, et al. 2D interactions and binary crystals of dipolar and quadrupolar nematic colloids. *Phys Rev Lett*. 2008;100:217803.
- [40] Puschel-Schlotthauer S, Meiwes Turrión V, Hall CK, et al. The impact of colloidal surface-anchoring on the smectic A phase. *Langmuir*. 2017;33:2222–2234.
- [41] Blanc C, Kleman M. The confinement of smectics with a strong anchoring. *Euro Phys J E*. 2001;4:241–251.

- [42] Zuhail KP, Dhara S. Temperature dependence of equilibrium separation and lattice parameters of nematic boojum-colloids. *Appl Phys Lett*. 2015;106:211901.
- [43] Poulin P, Cabuil V, Weitz DA. Direct measurement of colloidal forces in an anisotropic solvent. *Phys Rev Lett*. 1997;79:4862.
- [44] Fukuda JI, Yokoyama H. Separation-independent attractive force between like particles mediated by nematic-liquid-crystal distortions. *Phys Rev Lett*. 2005;94:148301.
- [45] Tkalec U, Ravnik M, Zumer S, et al. Vortexlike topological defects in nematic colloids: chiral colloidal dimers and 2D crystals. *Phys Rev Lett*. 2009;103:127801.
- [46] Tkalec U, Muševič I. Topology of nematic liquid crystal colloids confined to two dimensions. *Soft Matter*. 2013;9:8140–8150.
- [47] Zuhail KP, Dhara S. Effect of temperature and electric field on 2D nematic colloidal crystals stabilised by vortexlike topological defects. *Soft Matter*. 2016;12:6812–6816.
- [48] Stannarius R, Harth K. Defect interactions in anisotropic two-dimensional fluids. *Phys Rev Lett*. 2016;117:157801.
- [49] Stannarius R, Harth K. Inclusions in freely suspended smectic films. *Liquid crystals with nano and microparticles*. In: Lagerwall JP, Giusy Scalia, editors. World Scientific. Luxembourg; Vol-I, 2017. p. 361–414.
- [50] Dolganov PV, Cluzeau P, Dolganov VK. Interaction and self-organization of inclusions in two-dimensional free-standing smectic films. *Liq Cryst Rev*. 2019;7:1–29.
- [51] Dolganov PV, Dolganov VK. Director configuration and self-organization of inclusions in two-dimensional smectic membranes. *Phys Rev E*. 2006;73:041706.
- [52] Patricio P, Tasinkevych M, Telo da Gama MM. Colloidal dipolar interactions in 2D smectic-C films. *Eur Phys J E*. 2002;7:117–120.
- [53] Gim MJ, Beller DA, Yoon DK. Morphogenesis of liquid crystal topological defects during the nematic-smectic A phase transition. *Nat Commun*. 2016;8:15453.
- [54] Turner MS, Sens P, Pincus P. Particulate inclusions in a lamellar phase. *Phys Rev E*. 1997;55:4394.
- [55] Santangelo CD, Kamien RD. Bogomol'nyi, prasad, and sommerfeld configurations in smectics. *Phys Rev Lett*. 2003;91:045506.
- [56] Tovkach OM, Fukuda JI, Lev BI. Peculiarity of the interaction of small particles in smectic liquid crystals. *Phys Rev E*. 2013;88:052502.
- [57] Schiller P. Indirect interaction of colloidal particles adsorbed on smectic films. *Phys Rev E*. 2000;62:918.
- [58] Turner MS, Sens P. Interactions between particulate inclusions in a smectic-A liquid crystal. *Phys Rev E*. 1997;55:R1275.
- [59] Rasi M, Zuhail KP, Roy A, et al. N- sm A- sm C phase transitions probed by a pair of elastically bound colloids. *Phys Rev E*. 2018;97:032702.
- [60] Bohley C, Stannarius R. Energetics of 2D colloids in free-standing smectic-C films. *Eur Phys J E*. 2006;20:299–308.
- [61] Silvestre NM, Patricio P. Elliptical soft colloids in smectic-C films. *Phys Rev E*. 2006;74:021706.
- [62] Dolganov PV, Nguyen HT, Joly G, et al. Shape of nematic droplets in smectic membranes. *Euro Phys Lett*. 2007;78:66001.
- [63] Gvozdozskyy I, Jampani VS, Škarabot M, et al. Light-induced rewiring and winding of Saturn ring defects in photosensitive chiral nematic colloids. *Eur Phys J E*. 2013;36:97.
- [64] Lintuvuori JS, Stratford K, Cates ME, et al. Colloids in cholesterics: size-dependent defects and non-Stokesian microrheology. *Phys Rev Lett*. 2010;105:178302.
- [65] Lintuvuori JS, Marenduzzo D, Stratford K, et al. Colloids in liquid crystals: a lattice boltzmann study. *J Mater Chem*. 2010;20:10547–10552.
- [66] Senyuk B, Lavrentovich OD, Smith CJ, et al. Rotation of solid spherical particles moving through a cholesteric liquid crystal. In 22nd International Liquid Crystal Conference, Jeju, Korea, 2008 (Genicom Co., Ltd., Daejeon, 2008).
- [67] Jampani VS, Škarabot M, Ravnik M, et al. Colloidal entanglement in highly twisted chiral nematic colloids: twisted loops, hopf links, and trefoil knots. *Phys Rev E*. 2011;84:031703.
- [68] Senyuk B, Puls O, Tovkach M, et al. Hexadecapolar colloids. *Nat Commun*. 2016;7:1–7.
- [69] Senyuk B, Liu Q, He S, et al. Topological colloids. *Nature*. 2013;493:200–205.
- [70] Yuan Y, Liu Q, Senyuk B, et al. Elastic colloidal monopoles and reconfigurable self-assembly in liquid crystals. *Nature*. 2019;570:214–218.